Photoinduced Reactivity of Liquid Ethanol at High Pressure

Matteo Ceppatelli, Samuele Fanetti, Margherita Citroni, and Roberto Bini*

LENS, European Laboratory for Nonlinear Spectroscopy, Via N. Carrara 1, I-50019 Sesto Fiorentino, Firenze, Italy, and Dipartimento di Chimica dell'Università degli Studi di Firenze, Via della Lastruccia 3, I-50019 Sesto Fiorentino, Firenze, Italy

Received: July 14, 2010; Revised Manuscript Received: September 13, 2010

The room temperature photoinduced reactivity of liquid ethanol has been studied as a function of pressure up to 1.5 GPa by means of a diamond anvil cell. Exploiting the dissociative character of the lowest electronic excited states, reached through two-photon absorption of near-UV photons (350 nm), irreversible reactive processes have been triggered in the pure system. The active species are radicals forming along two main dissociation channels involving the split of C−O and O−H bonds. The characterization of the reaction products has been performed by in situ FTIR and Raman spectroscopy. At pressures of a few megapascals, molecular hydrogen is the main reaction product, an important issue in the framework of environmentally friendly synthesis of this energetic vector. In the gigapascal range, the main products are ethane, 2-butanol, 2,3-butanediol, 1,1-diethoxyethane, and some carbonylic compounds. The relative amount of these species changes with pressure reflecting the nature of the radicals formed in the photodissociation process. As the pressure increases, the processes requiring a greater molecularity are favored, whereas those requiring internal rearrangements are inhibited. Disproportion products like CH_4, H_2O, and CO_2 increase when the amount of ethanol decreases due to the reaction, becoming the main products only when ethanol is exhausted.

1. Introduction

The molar volume of a molecular system can be efficiently reduced by the application of a suitable external pressure. Any molecular compound, including the simplest diatomics, exhibits a change of the structural and physical properties with increasing density.[1] This is a consequence of the progressive alteration of the electronic density distribution that can be pushed up to induce a chemical instability of the system.[2] Association processes are generally expected and the pressure range where such phenomena are observed depends on the molecular stability, varying from a few gigapascals for the simplest unsaturated molecules like ethylene[3] or acetylene[4] to hundreds of gigapascals as in the case of nitrogen.[5] In many cases, catalytic concentrations of electronically excited molecules, attainable through two-photon (TP) absorption processes, have been shown to significantly lower these thresholds pressures for the chemical transformation.[6] Benefiting from the high density conditions, the electronic and geometrical changes characteristic of the electronically excited molecule can indeed efficiently trigger a chemical reaction. This is a remarkable finding because the lowering of the reaction threshold pressure can make these syntheses, where only physical methods are employed, appealing for environmentally friendly applicative purposes.[7]

Within this framework, an interesting class of reactions is that involving molecular species that, once properly activated by optical excitation, can trigger a chemical reaction in a host material otherwise stable at the $P-T$ conditions of the experiment. For example, water was recently employed to trigger chemical reactions in fluid mixtures and hydrates of simple molecules like N_2 and CO[8] and small hydrocarbons like acetylene and ethane.[9] The lowest electronic excited states of water, having dissociative character, were reached through two-photon absorption of near-UV photons and the radicals generated were used to trigger a chemical reaction in the host material. The formation of hydrogen was a remarkable result, making this class of reactions of interest also from energetic point of view. An analogous dissociative character of the lowest electronic excited states characterizes also the simplest alcohols like methanol and ethanol.[10,11] The homolytic split of the hydroxyl OH bond, leading to the methoxide and ethoxide radicals formation, has been identified as the main dissociation channel, whereas a secondary, but important channel, is the formation of the hydroxyl radical. The possible chemical processes activated by these radical species are of particular interest especially as the hydrogen synthesis is concerned. Ethanol is indeed an ideal candidate for pollution-free H_2 generation because it is a renewable source that would allow a net-zero CO_2 emission.[12,13] In fact, more than 90% of H_2 is currently produced by natural gas or light oil fraction and is therefore associated with the emissions of greenhouse gases and pollutants. Steam reforming of ethanol is for example a promising choice, even though the formation of undesired byproducts like methane and CO represents an important drawback.[14] The photocatalytic ethanol splitting is another promising clean source of H_2. This approach, already well established in the case of water,[15,16] is based on the absorption of visible light by a suitable semiconductor to generate electrons and holes in the conduction and valence bands, respectively. Water molecules are reduced by the electrons giving H_2 and are oxidized by the holes to give O_2. In this framework, the employment of solar light, a target in sustainable energy scenarios because of the delocalization of energy production to reduce the costs and the eco-impact of fuel transportation, in combination with renewable materials such as ethanol is an exciting perspective.[17]

* Corresponding author. Tel. +39-055-4572489 (4573079). Fax: +39-055-4572451. E-mail: roberto.bini@unifi.it.

10.1021/jp106516t
Published on Web 11/05/2010

Here we show how pure liquid ethanol can be successfully dissociated by two-photon absorption of near-UV photons. A complex reactivity, depending on pressure and on the reactant amount, leads to the formation of a few specific products among which hydrogen has to be remarked especially for the mild pressure conditions required for its synthesis.

2. Experimental Section

A membrane diamond anvil cell (MDAC) equipped with IIa type diamonds was employed to contain and pressurize the ethanol samples. Gilded stainless steel gaskets were used to ensure chemical inertness. The gaskets were first indented to about 50 μm thickness and then drilled to produce a 200 μm diameter hole. The hole was filled with gold, pressed, and then drilled again to produce a sample chamber of about 150 μm in diameter. Fresh ethanol by Fluka (99.8%) was loaded together with a small ruby chip for pressure calibration by the ruby fluorescence method. The energy threshold for the photoinduced reaction was searched by performing irradiation cycles of several hours using the emission lines (514.5, 488, 476.5, 457.9, and 350 nm) of an Ar ion laser with power ranging from 60 to 450 mW, taking care to homogeneously irradiate the whole sample. Reactivity was observed only when the UV multiline emission (peaked at 350 nm) was focused onto the sample. Raman spectra were measured in a back scattering geometry by using 40−250 mW of the 647.1 nm line of a Kr^+ laser. The different regions of the sample could be probed with a spatial resolution of about 10 μm. The scattered light was dispersed by a single-stage monochromator (900 grooves/mm) and analyzed by a CCD detector with a resulting instrumental resolution of 0.7 cm^{-1}. FTIR absorption measurements were performed with a Bruker-IFS 120 HR spectrometer modified for high-pressure measurements.[18,19] The instrumental resolution was 1 cm^{-1}.

3. Results

The high-pressure photoinduced reactivity of liquid ethanol was studied at room temperature as a function of pressure, irradiation power, and wavelength. Liquid ethanol is stable in all the investigated pressure range ($P < 1.7$ GPa) under several hours (5−10 h) of laser irradiation (500 mW) using wavelength $\lambda \geq 458$ nm. Reactivity was observed when the sample was irradiated with laser light at 350 nm and power exceeding 100 mW. All the experiments were performed in the DAC, and the laser beam was focused in order to fully and homogeneously irradiate the samples (~150 μm diameter). In this way, diffusion processes in the liquid can be reasonably neglected. In order to reproduce the experimental conditions of the higher pressure experiments and to guarantee a perfect sealing of the reaction chamber, mandatory for the spectroscopic analysis of the product, also the experiments close to room pressure were performed in the DAC allowing the obtainment of pressures as low as some MPa. In these latter cases, after ethanol was loaded into the cell the helium gas pressure in the membrane was slowly increased to approximately half of the indenting pressure. In most of the attempts the sample was not sealed in these conditions, with its consequent loss. The presence of the sample was verified by FTIR and Raman spectra that were always measured before the compression or irradiation cycles. In these low-pressure experiments the sample pressure was too low to be determined by the usual ruby fluorescence method and, as will be discussed in the following, we used the C−H symmetric stretching vibration of methane (ν_1) formed in the reaction as pressure calibrant. The frequency shift of this mode has been indeed carefully studied as a function of pressure ($P \leq 300$ bar) along several isotherms.[20] No visual or spectral changes were detected in the sample after 5 h of irradiation either with 500 mW of the 458 nm or with 60 mW of the 350 nm laser lines. On the contrary, a small gas bubble appeared in the sample after 5 h of irradiation with 160 mW of the 350 nm laser line, indicating the occurrence of a reaction (Figure 1a). A bubble of larger dimensions was obtained by irradiating a freshly loaded sample with 265 mW at 350 nm for the same amount of time (Figure 1b). In both cases the bubble composition was investigated by Raman spectroscopy and it resulted to be essentially composed by molecular hydrogen (Figure 1). The Raman spectra show the characteristic rotational bands of H_2 at 354 ($S_0(0)$), 586 ($S_0(1)$), 814 ($S_0(2)$), and 1033 ($S_0(3)$) cm^{-1},[21] and the Q lines at 4127 ($Q_1(3)$), 4144 ($Q_1(2)$), 4155 ($Q_1(1)$) and 4161 ($Q_1(0)$) cm^{-1}.[22] In addition, weaker bands allow for the identification of methane (2916 cm^{-1}) and ethane (993, 2897, and 2953 cm^{-1}).[23,24] The methane band at 2916 cm^{-1} was used as pressure calibrant.[20] Pressures of 4.7(2) (2916.67(3) cm^{-1}) and 7.2(2) (2916.14(3) cm^{-1}) MPa were measured in the case of the irradiations performed with 160 and 265 mW, respectively. Raman spectra of the homogeneous transparent region surrounding the bubbles do not show other bands than those of ethanol. On the contrary, FTIR spectra reveal weak absorption bands of additional reaction products in the spectral regions not obscured by the saturated absorptions of ethanol and diamond. In Figure 2 the four significant accessible spectral regions are shown before and after the irradiation. The presence of methane, revealed by the Raman spectrum, is confirmed by the weak absorption at 1303 cm^{-1} due to the IR active bending mode ν_4. In addition, the formation of CO_2 is evidenced by the absorption of the asymmetric stretching mode at 2339 cm^{-1}. Several other bands can be identified between 900 and 1020 cm^{-1} and between 1600 and 1800 cm^{-1}. These complex absorption patterns were deconvoluted by pseudo-Voigt profiles as shown in two examples reported in Figure 3. The broad absorption band at 1640 cm^{-1} was assigned to the bending mode of water.

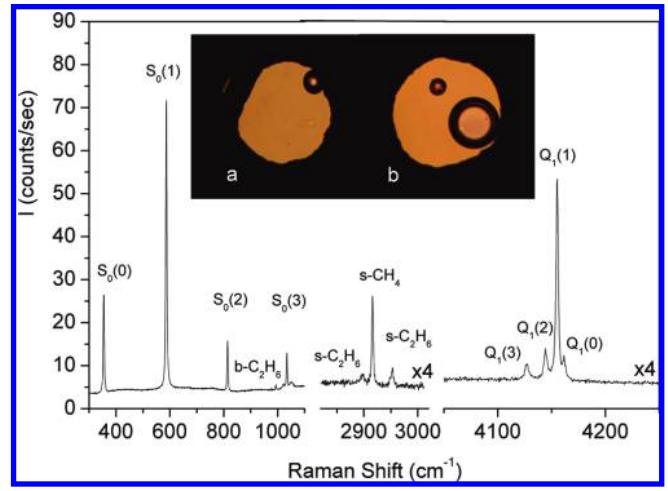

Figure 1. Microphotographs of the sample after 5 h irradiation using a UVML laser emission peaked at 350 nm with (a) 160 mW and (b) 265 mW. The small dark circle in sample b is the ruby chip, not present in sample a. The Raman spectra reported in the figure were measured in the bubble of sample b. The bands labeled as $S_0(i)$ and $Q_1(i)$ are the rotational and rotovibrational Q lines of H_2, respectively. The bands relative to the bending (b-C_2H_6) and C−H stretching (s-C_2H_6) modes of ethane, as well as that corresponding to the C−H stretching mode of methane, are also indicated. The pressure of the two samples was determined by the frequency of the C−H stretching mode of methane: (a) 4.7 MPa and (b) 7.2 MPa.

In two higher pressure experiments, at 0.5 and 1.0 GPa, we performed several irradiation cycles in order to carefully study

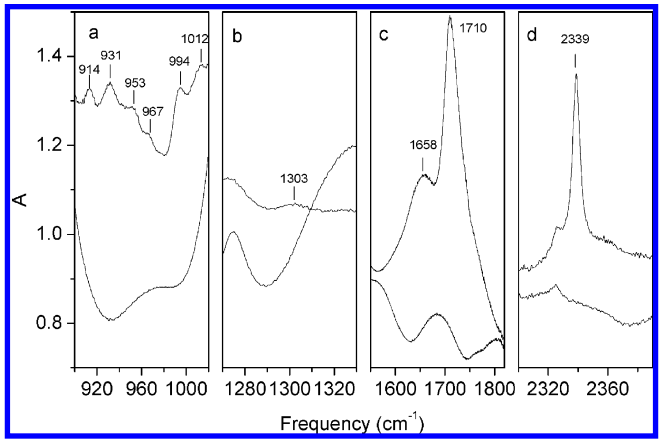

Figure 2. FTIR spectra measured in the spectral regions not masked by the ethanol and diamond absorptions at 7.2 MPa before (lower trace) and after (upper trace) 5 h of irradiation with 265 mW of the UVML laser emission peaked at 350 nm.

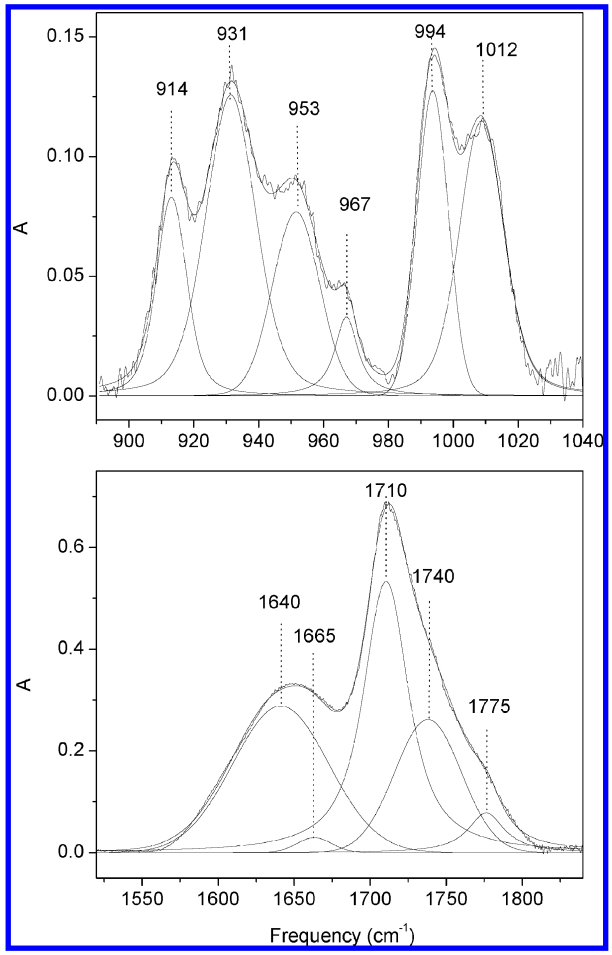

Figure 3. Deconvolution of the IR absorption regions reported in panels a and c of Figure 2 after baseline linearization.

the reaction evolution with the irradiation time. These experiments, besides providing useful information about the formation sequence of the different products, were very important for their identification. The sample remained almost homogeneous and transparent even after about 20 h of irradiation. After further irradiation, gray regions appeared in the sample which, successively, assumed a heterogeneous appearance with bubbles and dark and reddish regions (Figure 4). The evolution of the IR absorption spectrum with irradiation time at 1.0 GPa is reported in Figure 5. It can be readily appreciated that the four absorption regions analyzed behave differently with irradiation, thus indicating the existence of different reaction paths. In the lower frequency region, the complex absorption pattern shows a rapid intensification during the first hours of irradiation and a decrease after 10 h. The products bands in the 1600−1800 cm^{-1} frequency region, on the contrary, grow steadily with the irradiation time, exhibiting a sharp increase during the last cycle when also the bands of CH_4 (1301 cm^{-1}) and CO_2 (2340 cm^{-1}) show an abrupt intensification. The evolution of the integrated absorptions with irradiation time clearly shows this different behavior, especially when compared to the consumption rate of ethanol (Figure 6). The latter is in fact almost constant during the entire experiment in contrast to the integrated absorption maximum shown around 10 h of irradiation by the species responsible for the low-frequency bands (900−1020 cm^{-1}), and with the sudden growth of the higher frequency absorption bands (1600−1800 cm^{-1}). These differences clearly indicate that we are observing the formation of several reaction products and reveal the existence of different reaction channels.

The Raman spectrum is also extremely informative, showing the presence of many bands due to reaction products. As an example, the spectrum measured after 13 h irradiation at 0.5 GPa is reported in Figure 7. A careful Raman analysis of different sample regions evidenced an almost homogeneous composition. Raman spectra could not be measured after longer irradiation times because of a strong fluorescence background likely ascribable to the presence of the colored products (Figure 4). The material quenched at ambient conditions after 42 h of irradiation and further decompression appeared as a dark solid whose IR spectrum is reported in Figure 8.

A higher pressure experiment, just below the melting at 1.5 GPa, was performed by using a slightly higher laser power (450 mW). In this case, the sample readily reacted after 2 h of irradiation, showing the bands of methane, water, and carbon dioxide, whereas these species were observed in the lower pressure experiments only after 20 h irradiation.

4. Assignment of the Product Bands

With only few exceptions, where assignment of IR and Raman bands was straightforward (H_2, CO_2, CH_4, and H_2O), the identification of the reaction products required a careful analysis of the spectra. First, we tried to identify the IR bands showing the same behavior with irradiation time. As already mentioned, this procedure allowed for the uncoupling of the products responsible for the absorptions in the regions 900−1020 cm^{-1} and 1600−1800 cm^{-1}. The bands detected in the latter region, due to the water bending and carbonyl stretching modes, intensify continuously with irradiation not having a counterpart in the lower frequency region (Figure 6). Among the six bands in which the complex absorption profile between 900 and 1020 cm^{-1} can be deconvoluted (Figure 3), we identified three groups of bands which show an analogous intensification, or weakening, as a function of pressure (Figure 9) and of the irradiation time (Figure 6). The first group is composed of the two bands at 931 and 1012 cm^{-1} (low-pressure values), the second by the three bands at 914, 967, and 994 cm^{-1}, and the third by the band at 953 cm^{-1}, one of the weakest bands in the experiments performed at low pressure but intensifying with pressure to become the strongest after the irradiation at 1.5 GPa. This observation supports the assignment of these absorption bands to different products and marks the important role that pressure plays in selecting different reaction paths. Among the possible compounds attainable from chemical reactions involving the ethanol molecule, we selected those presenting IR bands

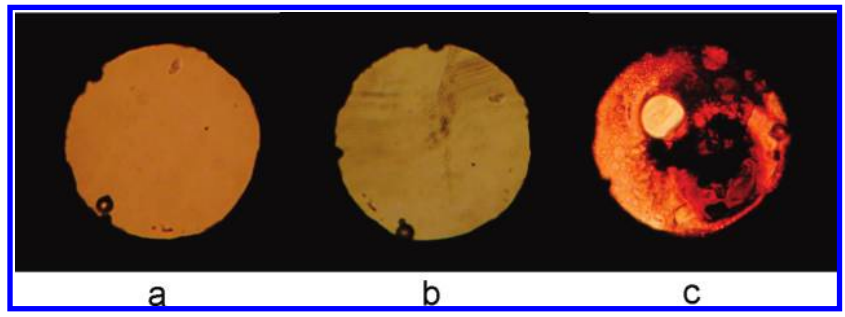

Figure 4. Microphotographs showing the changes occurring in the sample during the irradiation (265 mW, 350 nm) cycles at 0.5 GPa: (a) before irradiation, (b) after 27 h, and (c) after 42 h.

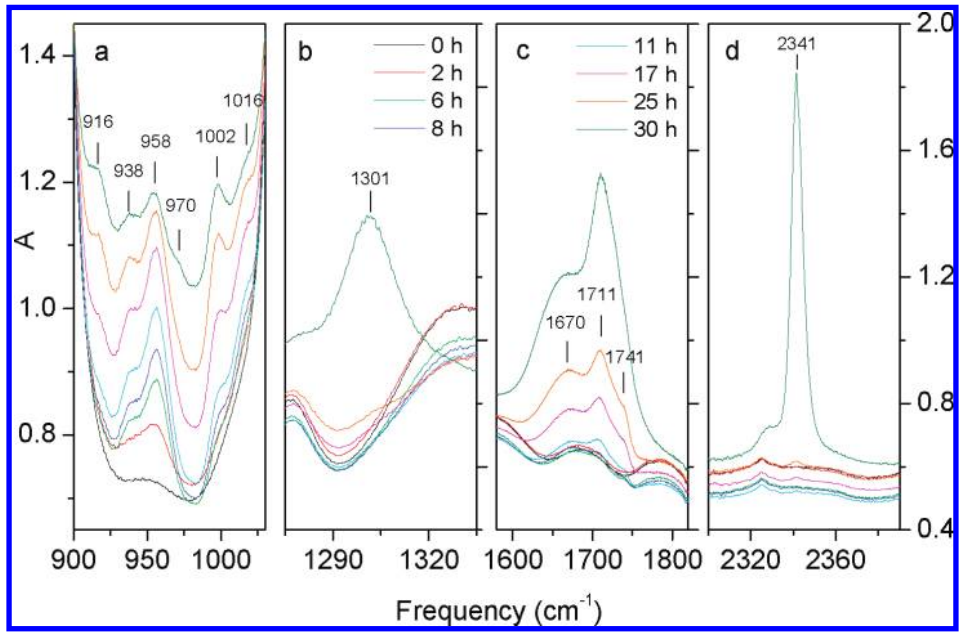

Figure 5. Evolution of the FTIR absorption spectrum with irradiation time (265 mW, 350 nm) in the experiment performed at 1.0 GPa. The vertical scale of panels b and c refers to the absorbance scale of panel d.

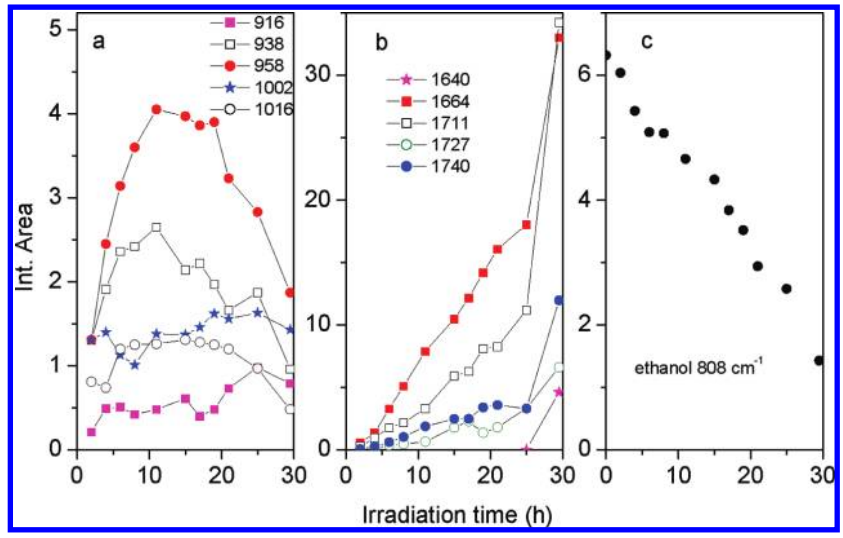

Figure 6. Evolution of the integrated absorption of some selected absorption bands with irradiation time (265 mW, 350 nm) at 1.0 GPa. Panel a, absorption bands in the 900−1020 cm^{-1} frequency range; panel b, absorption bands in the 1600−1800 cm^{-1} frequency range; panel c, ethanol band at 808 cm^{-1}. The ethanol band at 808 cm^{-1} has been chosen because it is isolated and not saturated also at the beginning of the experiment.

reproducing the frequency and the intensity ratio of the three groups identified. Then, the literature Raman spectra of the selected molecules were carefully compared to those measured during the photoinduced high-pressure reactions. An excellent agreement with the entire spectral information, frequency and relative intensities of both Raman and IR bands, is given only by three molecules: 2-butanol, 2,3-butanediol, and 1,1-diethoxyethane.

The deconvolution of the 1600−1800 cm^{-1} spectral region gives evidence of the existence of five other bands besides that

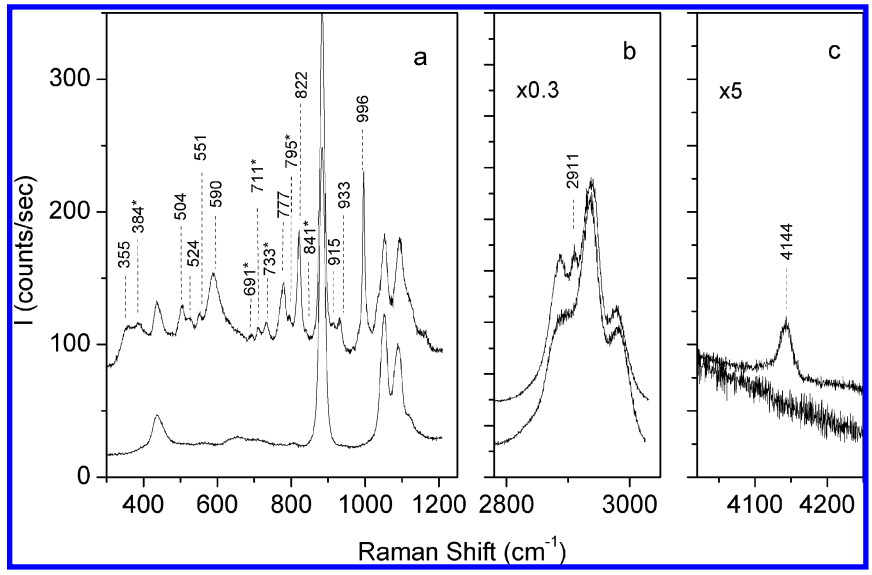

Figure 7. Lower traces: Raman spectra of ethanol measured at 0.5 GPa before irradiation. Upper traces: Raman spectra measured at the same pressure after 13 h of irradiation (265 mW, 350 nm). The asterisks indicate the product bands that were not assigned. The Raman intensities of panels b and c were scaled by a factor 0.3 and 5, respectively.

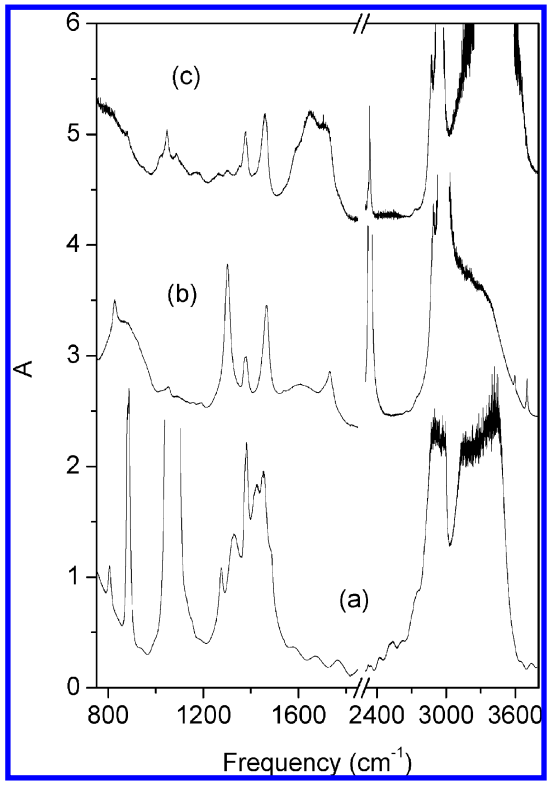

Figure 8. Comparison of the FTIR spectra measured (a) at 0.5 GPa before starting the irradiation cycles; (b) at 0.5 GPa after the irradiation completion (42 h, 265 mW, 350 nm); (c) after quenching at ambient conditions.

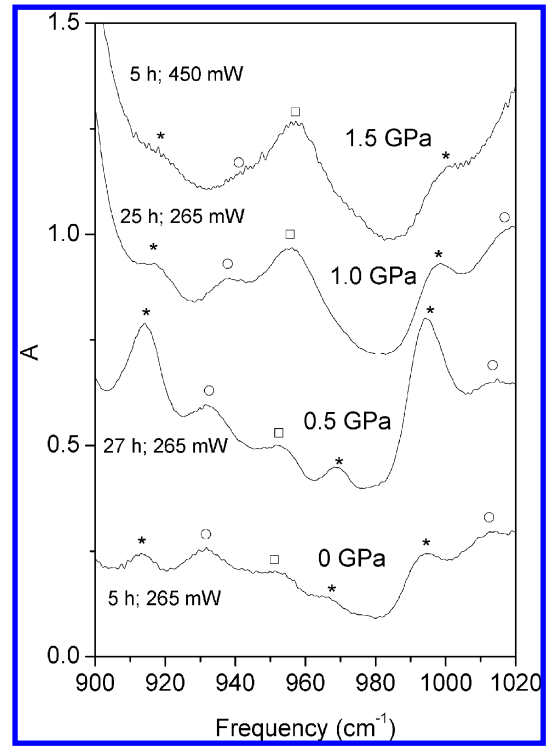

Figure 9. Comparison among the FTIR spectra collected during the different experiments in the 900−1020 cm^{-1} spectral region. The pressure of the experiment and the duration and the power of irradiation are indicated for each spectrum. Labels identify the bands of the products. Asterisks, 2-butanol; empty circles, 2,3-butanediol; empty squares, 1,1-diethoxyethane.

relative to the H_2O bending mode. The bands at 1665, 1710, and 1740 cm^{-1} are observed in all the experiments. The band at 1775 cm^{-1} is observed only at the lowest pressure, whereas in the higher pressure experiment a new absorption is detected at 1725 cm^{-1}. However, these bands cannot be related to other absorptions characterized by a similar evolution with irradiation time thus preventing a precise identification of the carbonylic compounds. The shape and the position of the broad band centered at 1665 cm^{-1} recalls the absorption of molecules presenting a stabilized enolic form, like β-diketone compounds, but a more precise assignment is prevented by the lack of additional information. On the basis of the literature reports concerning the chemistry of ethanol, we tentatively assigned the bands at 1710, 1725, and 1740 cm^{-1} to acetone, acetaldehyde, and ethyl acetate, respectively. The complete assignment is reported in Tables 1 and 2.

5. Discussion

Liquid ethanol was shown to be chemically unstable under irradiation with near-UV light (350 nm) giving rise to a complex

TABLE 1: IR Peak Frequencies (cm^{-1}) of the Product Bands and Their Assignment According to Literature Data

	ambient pressure	0.007 GPa	0.5 GPa	1.0 GPa	1.5 GPa
ethane	822[a]	822	822	826	828
methane	1306[a]	1303	1303	1301	1298[c]
2-butanol	914[a]	914	914	916	919
	968[a]	967	968	970	
	992[a]	994	994	1002	999
2,3-butanediol	929[a]	931	933	938	
	1011[a]	1012	1010	1016	
1,1-diethoxyethane	953[a]	953	958	957	957
acetone	1712[a]	1710	1710	1711	1715[c]
acetaldehyde	1727[b]		1725	1728	
ethyl acetate	1742[a]	1740	1742	1741	

[a] Reference 25. [b] Liquid film. [c] Estimated value from the saturating peak.

TABLE 2: Raman Peak Frequencies (cm^{-1}) of the Products Bands and Their Assignment According to Literature Data

	ambient pressure	0.007 GPa	0.5 GPa	1.0 GPa	1.5 GPa
hydrogen	354[a]	354	355		
	587[a]	586	590		
	814[a]	814			
	1034[a]	1033			
	4126[b]	4127			
	4143[b]	4143	4144		
	4155[b]	4155			
	4161[b]	4161			
ethane	995[c]	993	996	1001	1004
	2896[d]	2897			
	2954[c]	2953			
methane	2917[e]	2916	2911		2924[f]
2-butanol	502[d]		504	506	
	776[d]		777	783	
	819[d]	819	822	823	
	914[d]		915		
2,3-butanediol	525[d]		524		
	549[d]		551	553	
	929[d]		933	935	
1,1-diethoxyethane	529[d]			532	
	808[d]			810	

[a] Reference 21. [b] Reference 22. [c] Reference 23. [d] Reference 25. [e] Reference 20. [f] Here methane is crystalline (ref 26).

reactivity where several reaction channels can be identified. The existence of a threshold wavelength for the reaction was revealed by using different excitation wavelengths in the visible region down to 458 nm without observing any chemical alteration of the sample. The photoinduced reaction was also extremely sensitive to the incident power, revealing the chemical transformation only above 100 mW, corresponding to an irradiance of $\sim$0.6 kW/cm^2. This is readily explained by considering that at ambient conditions the lowest absorption band of ethanol, due to the n $\rightarrow \sigma^*$ Rydberg transition,[27,28] is centered at 8.38 eV (148 nm) with the onset at about 6.9 eV (180 nm).[29] The electronic excitation of ethanol was therefore realized through a two-photon absorption process. Although a characterization of the electronic excited states of ethanol is to our knowledge not available, the strong similarities between the electronic structures of ethanol and methanol, reflected in the almost identical absorption spectra and differing only for a small red shift in the methanol case,[29] suggest a similar character of the excited states. These observations are supported by the analogous dissociation behavior following excitation at 193.3 nm reported for the two systems.[10,11] Experimental and theoretical studies evidenced that the lowest excited state of methanol is dissociative along the CH_3O-H coordinate and weakly bonding along the CH_3-OH one.[30] The dissociation leading to the formation of the ethoxy radical has been identified as the primary photodissociation channel at 193.3 nm also in jet-cooled ethanol.[11]

The relative weight of the reactive paths evidenced in this study depends both on pressure and on irradiation time. Three groups of reactions can be roughly identified on the basis of the products formed during the irradiation cycles. The first regards the formation of hydrogen, ethane, 2-butanol, 2,3-butanediol, and 1,1-diethoxyethane. All these products are ascribable to reactions occurring in the first hours of irradiation when ethanol is in large excess and are likely initiated by radical species. The second group concerns with disproportion reactions, mainly occurring after a long irradiation time, and leading to formation of methane and carbon dioxide. These reactions are also presumably related to the limited amount of ethanol present in the reaction volume. The third group is related to the formation of water and carbonyl species which show a continuous increase with irradiation time, although a steeper increase of the reaction rate was observed when also the disproportion processes took place. This behavior suggests a complex chemistry initiated by radicals and evolving in successive addition/elimination processes involving also some products like 2-butanol, 2,3-butanediol, and 1,1-diethoxyethane whose concentration decreases for long irradiation time. These processes are likely responsible for the formation of the extended solid material recoverable at ambient conditions. It is worth mentioning that the ethanol reactivity is in this case rather different from that observed at high temperature[36,38] or that induced by multiphoton absorption of IR radiation.[31] In fact, in both cases the production of CO, methane, and H_2 is evidenced with the only significant difference concerning the formation of ethane and ethylene which are largely obtained in the thermal decomposition and in the IR photoinduced reactions, respectively.

Molecular hydrogen is the reaction product showing the highest sensitivity to the pressure conditions. This species is indeed the main product in the reactions performed at the lowest pressures, and is still detectable at 0.5 GPa, but no evidence of its formation was gained in the higher pressure experiments. The H_2 formation has to be related to the reaction between an ethanol molecule and the H atom produced in the photodissociation of the O−H bond.[32] This is an important confirmation that cleavage of the O−H bond is, at least at low pressure, the primary photodissociation process, as reported in ref 11 and in agreement with the results obtained for methanol, where the dissociation along the OH coordinate accounts for 86% of the dissociated species.[10] The absence of H_2 among the reaction products above 0.5 GPa indicates that new reaction channels open, or simply become more efficient, with rising density and that H atoms are efficiently captured by highly reactive intermediates. We roughly estimated the amount of hydrogen formed during the low-pressure reactions by measuring the bubbles dimensions and assuming they were entirely composed by H_2. This approach likely overestimated the H_2 amount because also traces of methane and ethane were detected by Raman spectroscopy. The volume of the sample could be determined quite precisely by measuring its diameter through a microscope and its thickness by the interference fringes in the FTIR spectrum. The amount of ethanol transformed during the photoreaction was calculated by assuming that at the end of the reaction the liquid part of the sample was still essentially composed by ethanol, whose density as a function of pressure

is reported in ref 33. The amount of hydrogen produced was computed by using the van der Waals law for real gases. The results of the calculations give 16 pmol h^{-1} of molecular hydrogen for the experiment at 7.2 MPa and 5.4 pmol h^{-1} for that at 4.7 MPa. The ratio in the hydrogen yield is 2.96 in excellent agreement with the expected value of 2.74 calculated on the basis of the quadratic dependence on the incident power, as expected for a dissociation process driven by two-photon absorption.[34]

As already mentioned, during the first hours of irradiation, besides molecular hydrogen, we observed the formation of ethane, 2-butanol, 2,3-butanediol, and 1,1-diethoxyethane. With the only exception of ethane none of these compounds has been reported in photoinduced or thermal reactions. In addition to the well-established split of the O−H bond, three other energetically possible photodissociation processes have been proposed after one-photon excitation at 193.3 nm in the gaseous phase:[11]

$$C_2H_5OH \rightarrow CH_3CH_2\dot{O} + \dot{H} \quad (\Delta H^\circ = 103.7 \text{ kcal/mol}) \tag{1}$$

$$C_2H_5OH \rightarrow CH_3\dot{C}H_2 + \dot{O}H \quad (\Delta H^\circ = 89.2 \text{ kcal/mol}) \tag{2}$$

$$C_2H_5OH \rightarrow CH_3\dot{C}HOH + \dot{H} \quad (\Delta H^\circ = 92.8 \text{ kcal/mol}) \tag{3}$$

$$C_2H_5OH \rightarrow \dot{C}H_2CH_2OH + \dot{H} \quad (\Delta H^\circ = 98 \text{ kcal/mol}) \tag{4}$$

Despite these mechanisms were derived for gaseous ethanol, the close resemblance between the absorption spectra of the gas and liquid phases[29] indicates that the energetics, and then the dissociation reactions, should not substantially differ. Ethane, barely detectable in the lower pressure experiments and always one of the main products at higher pressure, can readily form through hydrogenation of the radical produced in the dissociation process (2). This indicates the importance of this dissociation channel especially with increasing pressure. Both 2-butanol and 2,3-butanediol can form from the radical deriving from process (3) through the association with another radical of the same type, to give 2,3-butanediol, or with the ethyl radical forming 2-butanol. Nevertheless, the direct reaction of two radicals is an unlikely process because of the small TP cross sections, typically ≤10 Goeppert-Mayer (GM), that determines catalytic concentration of the dissociated species at the laser intensities employed in all the experiments. Therefore, the formation of 2-butanol and 2,3-butanediol can be reasonably addressed to processes involving a radical and ethanol molecules. The radical forming in process (3) is likely involved in the formation of these products despite the main dissociation product being, according to literature, the ethoxy radical. Nevertheless, the radical reported in process (3) can also derive from an internal rearrangement of the ethoxy radical to the most stable $CH_3\dot{C}HOH$ form. Finally, the formation of 1,1-diethoxyethane can be depicted as the direct reaction of two ethanol molecules with a radical deriving from processes (1) or (2). It is therefore not surprising that the relative amount of 1,1-diethoxyethane increases with rising pressure because a higher molecularity, favored by the density increase, is required for its formation. Moreover, the formation of 1,1-diethoxyethane is competitive with that of 2-butanol and 2,3-butanediol whose IR bands are barely visible in the higher pressure experiment (Figure 9). The latter result supports the hypothesis that the radical reported in process (3), responsible for the formation of 2-butanol and 2,3-butanediol, most likely derives from an internal rearrangement of the ethoxy radical, such a process being slowed or inhibited by the pressure increase.

This interpretation of the results points to identification of (1) and (2) as the only active dissociation channels. In fact, we do not have evidence of the formation of butanol or butanediol with the hydroxyl group in position 1 that should form through the radical produced in channel (4). Diethyl ether is another product obtainable from the dissociation channels (1) and (2) but not observed experimentally. However, it is reported to decompose under UV irradiation in the presence of oxidants like the OH radical.[35] Two of the carbonyl species proposed as possible products (Tables 1 and 2) can also be explained by the dissociation channels (1) and (2). When the ethoxy radical is produced in an excited vibrational state, it can lose another H atom, giving rise to acetaldehyde[11] that can further react with an ethoxy radical to give ethyl acetate.

Disproportion and decomposition species can derive both from ethanol and reaction products. This holds particularly for CO_2, whose formation in the thermal decomposition of ethanol has not been reported,[31,36] but also for methane, water, and carbonyl species (acetone) all exhibiting a similar behavior during the irradiation. At low pressure these compounds are already present after the first hours of irradiation. On the contrary, at 0.5 and 1.0 GPa they steeply increase in the last irradiation hours, while ethanol keeps the same transformation rate and the bands assigned to the alcoholic products slightly decrease. This suggests that at low density the radical species formed in the photodissociation of ethanol preferentially evolve toward fragmentation processes originating a complex chemistry where the hydroxyl radical plays a key role as attested by the abundance of oxidation products. The identification of methane as a disproportion product is also important to rule out the possible dissociation along the C−C bond which would represent a major difference with respect to the gas phase dissociation mechanisms.

When ethanol is almost, or completely, finished, the decomposition processes become dominant involving the reaction products that, in turn, could be photodissociated along reactive paths similar to those of ethanol. Besides H_2O, CO_2, CH_4, and acetone, a solid carbonaceous material, likely due to the association of the pre-existent aliphatic chains, is the ultimate product of the reaction. As a matter of fact, the IR absorption spectrum of this material closely recalls those of long-chain saturated primary alcohols. The assignment of the main IR absorption bands (Figure 8) is indeed quite straightforward: the saturated band at ∼3400 cm^{-1} to the O−H stretching mode, the band at 2940 cm^{-1} to the C−H stretching, the doublet at 1458 and 1377 cm^{-1} to the asymmetric and symmetric CH_3 bending, and finally the peak at 1047 cm^{-1} to the C−C−O stretching of primary alcohols. Three different overlapped bands are observed in the carbonyl stretching region but their frequencies are not selective thus preventing the identification of the corresponding chemical species. The brownish coloration of the recovered solid suggests the presence of conjugation in agreement with the high hydrogen and oxygen content of the final stable molecular products.

6. Conclusion

Two-photon absorption of near-UV radiation triggers a complex reactivity in pure liquid ethanol even close to ambient

conditions. The dissociative character of the lowest electronic excited states allows for the generation of radicals that, exploiting the high-density conditions attainable with increasing pressure, are able to trigger a chemical reaction with the neighboring molecules. At pressures of a few megapascals a remarkably high amount of molecular hydrogen forms (tens of pmol at 0.8 kW/cm^2 irradiance), supporting the split of the O−H bond as the main dissociative channel. It should be remarked that only light and possibly pressure are employed for its synthesis. As the pressure is increased, several other products, barely detectable at low pressure, can be identified: ethane, 2-butanol, 2,3-butanediol, 1,1-diethoxyethane, some carbonylic compounds and the disproportion products CH_4, H_2O, and CO_2. Disproportion products appear essentially when the amount of ethanol is strongly reduced, thus suggesting that their formation takes place at the expense of the association products and that their formation could be controlled by working in large excess of ethanol. The split of the C−O bond, indicated as a minor dissociation path in the case of methanol, is found here to be extremely important. Ethane, and likely 1,1-diethoxyethane, are formed through the ethyl radical and their considerable amount in all the experiments, lowest pressure aside, marks the importance of this channel as the pressure is increased. Thus, the pressure increase favors the association products produced in the processes occurring through a greater molecularity and partly inhibits those where internal rearrangements are required. A solid recoverable brownish material forms along with the gaseous disproportion products. It appears mainly constituted by long aliphatic chain primary alcohols where different types of carbonyl groups and unsaturation are present. Further studies are mandatory to provide a better insight on two major issues outlined in this work. Careful quantitative measurements regarding the effect of pressure on the amount of H_2 produced would elucidate the potentiality of this method for applicative purposes. In addition, the study of the reaction employing deuterated isotopomers could allow a better definition of the reaction pathways.

Acknowledgment. This work was supported by the European Union under Contract RII3-CT2003-506350, given by the Italian Ministero dell'Università e della Ricerca Scientifica e Tecnologica (MURST), and by "Firenze Hydrolab" through a grant by Ente Cassa di Risparmio di Firenze.

References and Notes

(1) Hemley, R. J. *Annu. Rev. Phys. Chem.* **2000**, *51*, 763–800.
(2) Schettino, V.; Bini, R.; Ceppatelli, M.; Ciabini, L.; Citroni, M. Chemical reactions at very high pressure. In *Advances in Chemical Physics*; Rice, S. A., Ed.; Wiley: New York, 2005; Vol. 131, pp 105−242.
(3) Chelazzi, D.; Ceppatelli, M.; Santoro, M.; Bini, R.; Schettino, V. *Nat. Mater.* **2004**, *105*, 470–475.
(4) Ceppatelli, M.; Santoro, M.; Bini, R.; Schettino, V. *J. Chem. Phys.* **2000**, *113*, 5991–6000.
(5) Eremets, M. I.; Gavriliuk, A. G.; Trojan, I. A.; Dzivenko, D. A.; Boehler, R. *Nat. Mater.* **2004**, *3*, 558–563.
(6) Bini, R. *Acc. Chem. Res.* **2004**, *37*, 95–101.
(7) Anastas, P.; Warner, J. *Green Chemistry: Theory and Practice*; Oxford University Press: New York, 1998.
(8) Ceppatelli, M.; Bini, R.; Schettino, V. *Proc. Natl. Acad. Sci. U.S.A.* **2009**, *106*, 11454–11459.
(9) Ceppatelli, M.; Bini, R.; Schettino, V. *J. Phys. Chem. B* **2009**, *113*, 14640–14647.
(10) Satyapal, S.; Park, J.; Bersohn, R.; Katz, B. *J. Chem. Phys.* **1989**, *91*, 6873–6879.
(11) Xu, K. S.; Amaral, G.; Zhang, J. S. *J. Chem. Phys.* **1999**, *111*, 6271–6282.
(12) Navarro, R. M.; Sánchez-Sánchez, M. C.; Alvarez-Galvan, M. C.; Del Valle, F.; Fierro, J. L. G. *Energy Environ. Sci.* **2009**, *2*, 35–54.
(13) Ni, M.; Leung, D. Y. C.; Leung, M. K. H. *Int. J. Hydrogen Energ.* **2007**, *32*, 3238–3247.
(14) Haryanto, A.; Fernando, S.; Murali, N.; Adhikari, S. *Energy Fuels* **2005**, *19*, 2098–2106.
(15) Kudo, A.; Miseki, Y. *Chem. Soc. Rev.* **2009**, *38*, 253–278.
(16) Khaselev, O.; Turner, J. A. *Science* **1998**, *280*, 425–427.
(17) Ampelli, C.; Centi, G.; Passalacqua, R.; Perathoner, S. *Energy Environ. Sci.* **2010**, *3*, 292–301.
(18) Bini, R.; Ballerini, R.; Pratesi, G.; Jodl, H. J. *Rev. Sci. Instrum.* **1997**, *68*, 3154–3160.
(19) Gorelli, F. A.; Santoro, M.; Ulivi, L.; Bini, R. *Phys. Rev. Lett.* **1999**, *83*, 4093–4096.
(20) Lin, F.; Bodnar, J.; Becker, S. P. *Geochim. Cosmochim. Ac.* **2007**, *71*, 3746–3756.
(21) Ulivi, L.; Zoppi, M.; Gioè, L.; Pratesi, G. *Phys. Rev. B* **1998**, *58*, 2383–2386.
(22) Sharma, S. K.; Mao, H. K.; Bell, P. M. *Phys. Rev. Lett.* **1980**, *44*, 886–888.
(23) Lee, M. R.; Benamotz, D. *J. Chem. Phys.* **1993**, *99*, 10074–10077.
(24) Hansen, S B.; Berg, R. W.; Stenby, E. H. *Appl. Spectrosc.* **2001**, *55*, 55–60.
(25) Schrader, B. *Raman/IR Atlas of Organic Compounds*, 2nd ed.; VCH-Verlag-Ges.: Weinheim, Germany, 1989.
(26) Hebert, P.; Polian, A.; Loubeyre, P.; Le Toullec, R. *Phys. Rev. B* **1987**, *36*, 9196–9201.
(27) Salahub, D. R.; Sandorfy, C. *Chem. Phys. Lett.* **1971**, *8*, 71–74.
(28) Bonang, C. C.; Anderson, D. J.; Cameron, S. M.; Kelly, P. B.; Getty, J. D. *J. Chem. Phys.* **1993**, *99*, 6245–6252.
(29) Jung, J. M.; Gress, H. *Chem. Phys. Lett.* **2002**, *359*, 153–157.
(30) Cheng, B. M.; Bahou, M.; Chen, W. C.; Yui, C. H.; Lee, L. C.; Lee, Y. P. *J. Chem. Phys.* **2002**, *117*, 1633–1640.
(31) De Andrade Leite, S. R.; Isolani, P. C.; Riveros, J. M. *Can. J. Chem.* **1984**, *62*, 1380–1384.
(32) Jha, K. N.; Freeman, G. R. *J. Chem. Phys.* **1972**, *57*, 1408–1414.
(33) Papaioannou, D.; Zlakas, D.; Panayiotou, C. *J. Chem. Eng. Data* **1991**, *36*, 35–39.
(34) Demtröder, W. In *Laser Spectroscopy: Basic Concepts and instrumentation*, 3rd ed.; Springer-Verlag: Berlin, 2003.
(35) Wallington, T. J. *Environ. Sci. Technol.* **1991**, *25*, 410–415.
(36) Park, J.; Zhu, R. S.; Lin, M. C. *J. Chem. Phys.* **2002**, *117*, 3224–3231.
(37) Takiguchi, Y.; Uematsu, M. *J. Chem. Thermodyn.* **1996**, *28*, 7–16.
(38) Li, J.; Kazakov, A.; Dryer, F. L. *Int. J. Chem. Kinet.* **2001**, *33*, 859–867.
(39) Citroni, M.; Bini, R.; Foggi, P.; Schettino, V. *Proc. Natl. Acad. Sci. U.S.A.* **2008**, *105*, 7658–7663.

JP106516T